Photo-reversible solid to liquid transition of azobenzene containing polymers: Impact of the chemical structure and chain length

Laurence Pessoni, David Siniscalco, Anne Boussonniere, Anne-Sophie Castanet, Laurent Billon, Nicolas Delorme

Version of Record: https://www.sciencedirect.com/science/article/pii/S0014305722003019
Manuscript_ba8cbc101750210ee1f039718be7b546

Photo-reversible solid to liquid transition of azobenzene containing polymers: impact of the chemical structure and chain length.

Laurence Pessoni,[a,b*] David Siniscalco,[a] Anne Boussonnière,[a] Anne-Sophie Castanet,[a] Laurent Billon[b] and Nicolas Delorme[a*]

a Institut des Molécules et Matériaux du Mans (IMMM) – UMR CNRS 6283 – Le Mans Université, Avenue Olivier Messiaen, 72000 Le Mans, France

b Bio-Inspired Materials Group: Functionalities & Self-Assembly, Universite de Pau et des Pays de l'Adour, E2S UPPA, IPREM UMR 5254, 2 avenue Angot, 64000 Pau, France

*Corresponding Authors:
laurence.pessoni@univ-pau.fr and nicolas.delorme@univ-lemans.fr

Keywords: azobenzene • nitroxide mediated polymerization • azopolymer • isomerization• solid-to-liquid transition

Abstract

Azobenzene containing polymers (azopolymers) can exhibit a photo-reversible solid to liquid transition which is illustrated by a cyclic softening and hardening of the polymer material upon irradiation. In order to understand the structure–property relationship on this transition, Nitroxide Mediated Polymerization (NMP) was used for the first time to synthesize a series of azopolymers. Four azopolymers bearing various azobenzene groups were designed with different molecular weights. Photo-isomerization properties and photo-reversible solid-to-liquid transitions were studied as function of the molecular weight and structure of the azopolymers. It was found that molecular weights and chemical structure of the azopolymer have both an impact on the features of the reversible solid-to-liquid transition. In particular, the higher the length of the substituent or the linker, the faster the transition. The results obtained in this study help on the one hand to better understand the mechanism of the photo-reversible solid-to-liquid transition and on the other hand to consider the design of novel azopolymers for many applications.

1. Introduction

There is an increasing demand in the industry for smart materials and coatings that exhibit advanced properties as reversible responses to environmental changes,[1] including for example: temperature,[2] CO_2,[3,4] pH[5]. Light-responsive materials in which a quick and reversible response can be achieved are of particular interest. Indeed, light is a non-contact and mild energy source, which can be used specifically with regard to wavelength, intensity, or polarization direction to achieve precise and remote control.[6]

It has been known for years that depending of their molecular structure, azobenzene molecules and their derivatives can undergo reversible *trans* to *cis* isomerization upon irradiation with UV or visible light.[7–9] Azopolymers are well known for their efficient and robust photo-chemistry.[10] For these reasons, they have found applications in several fields[11] such as biomedical application,[12,13] in photoresponsive molecularly imprinted polymers (PMIPs),[14] actuators,[15,16] information storage,[17,18] solar energy storage,[19] or light-controlled microfluidics and other photonic devices.[20–23] Recently, it has been shown for some azopolymers that the reversible *trans-cis* photo-isomerization of the azobenzene moiety induces a reversible change on the mechanical properties of the material called Reversible Solid-to-Liquid Phase Transition (RSLPT) or photo-fluidization.[24–27] This transition is illustrated by a repeatable softening and hardening of the polymer material upon irradiation. Since then, the development of polymers with switchable mechanical properties has become an emerging research field in materials science and technology because of its potential applications such as adhesives,[25] self-healing materials,[28] photolithography[29,30] or anti-bacterial coating.[31]

Although, the RSLPT mechanism was rarely investigated,[26] the main hypothesis is that RSLPT is linked to a glass temperature variation during the *trans-cis* photo-isomerization. For polymers, RSLPT may occur when the processing temperature is between the glass transition temperature (*i.e. Tg*) of the *cis* form and that of the *trans* form. For instance, for an azopolymer with an acrylate backbone showing a RSLPT in ambient conditions, Zhou *et al.*[32] measured by DSC a decrease from Tg_{trans} = 48°C to Tg_{cis} = -10°C upon photo-isomerization.

Until now, only a few photo-sensitive polymers that undergo a RSLPT have been reported.[33] Most of these polymers are based on poly(meth)acrylates backbones [28,32,34–38] with azobenzene type molecules in the side chain. One of the reasons of the low number of available polymers that undergo RSLPT, is the strong influence of the azobenzene compounds structure on the isomerization properties. For example, Wu and co-workers in 2019[37] have shown that the azobenzene/polymer backbone spacer plays a major role in the RSLPT of poly(meth)acrylates azo homopolymers. Indeed, for short chain lengths, the *Tg* did not show a significant decrease after irradiation and the phase transition temperature was above room temperature for higher lengths. More recently, in 2020, Xu *et al.*[34] have demonstrated that the liquefaction rate of azopolymers drastically increased as the size of substituents increased. Despite these studies, there are still several critical issues or lack that need to be addressed in order to

further elucidate the correlation between the macromolecular features, *i.e.* nature of the azo-monomer, length of the polymer…. and the photo-responsiveness of azopolymers.

Properties of photoresponsive azopolymers depend indeed on their molecular weight and dispersity *Đ* values .[11] We have then chosen controlled radical polymerization CRP allowing simultaneously the control of the number-average molar mass, the dispersity and the chain end of polymer.[39] ATRP,[34–36,40,41] RAFT[32] or Cu(0)-RDRP[42] are used to polymerize azobenzenes bearing an acrylate or methacrylate as polymerizable group. RAFT polymerization can have a disadvantage for a photoisomerization study because usually a sulfur is present on the control agent and bring a yellow color to the final polymer, *i.e.* meaning an absorption in the UV-visible wavelength range. In ATRP polymerization, copper and an amine-based ligand are generally used as the catalyst. The removal of green-coloured copper bromide from the final polymer has to be done as previously described for coloured RAFT agent and is moreover tedious and time/cost consuming. So finally, NMP Polymerization reaction was chosen as simple to enforce experimentally, with only two species present in the reactor, the initiator and the monomer. To the best of our knowledge, no scientific paper reports the homopolymerization of azobenzene monomers by Nitroxide-Mediated Polymerization (NMP)[43] using an alkoxyamine (BlocBuilder®) as initiator. Only copolymerization with azobenzene in a small amount were described. Yoshida *et al.*[44] used NMP to copolymerize only 1 M% of styrenic azobenzene with BPO as initiator and 4-methoxy-TEMPO as a counter-radical. Srichan *et al.*[45] reported the copolymerization by NMP initiated by the BlocBuilder®, of a styrenic monomer with an initial 5 mol% *N*-substituted maleimide presenting an azobenzene substituent.

Herein, a series of azobenzene homopolymers with four different functional groups were synthetized by NMP to control the polymer chain length and dispersity, and finally study their influence on the RSLPT. We investigated the effect of alkyl- and alkoxy-based electron-donor groups, linkers length and polymer chain lengths on the photo-physical properties of the prepared azopolymers. Structure of monomers and polymers were characterized by ^{1}H NMR spectroscopy and the molecular weight/dispersity values of the polymers determined by size exclusion chromatography (SEC). The photoisomerization behavior in solution was followed by ^{1}H NMR in $CDCl_3$. Finally, the photoinduced liquefaction of the bulky polymers were studied by optical microscopy under UV irradiation.

2. Results and Discussion

2.1 Azomonomer synthesis.

The synthetic methodology for the azomonomers is represented in Scheme 1. The four azobenzene monomers were prepared from the corresponding hydroxyazobenzenes previously synthetized (See supplementary data “part 1”), with high yields (75 - 91 %) after purification (Table 4).

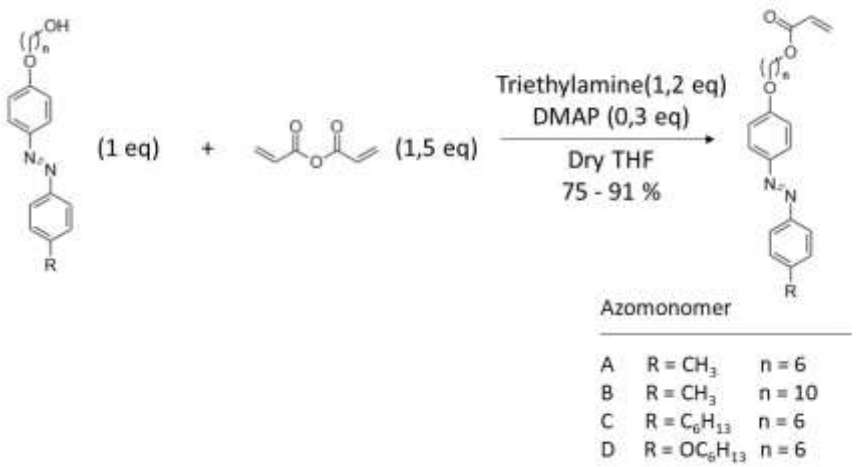

Scheme 1. *Synthetic methodology for azomonomers preparation.*

All monomeric chemical structures obtained were confirmed by ^{1}H NMR in $CDCl_3$ (supplementary data Figure S1 to S4 "part 2").

2.2 Azopolymerization by NMP.

All polymers were synthetized using NMP carried out at 115 °C. The polymerization was initiated by the BlocBuilder® alkoxyamine under control of the SG1 nitroxide radical. First, a kinetic study of the azomonomer "A" polymerization with a [M]/[I] of 14 and 27 was performed and each point of kinetics in `Figure 1 represents a monomer/initiator mixture splited from a "mother" solution without any purification process, *i.e.* precipitation (Table S1 in SI "part 2").

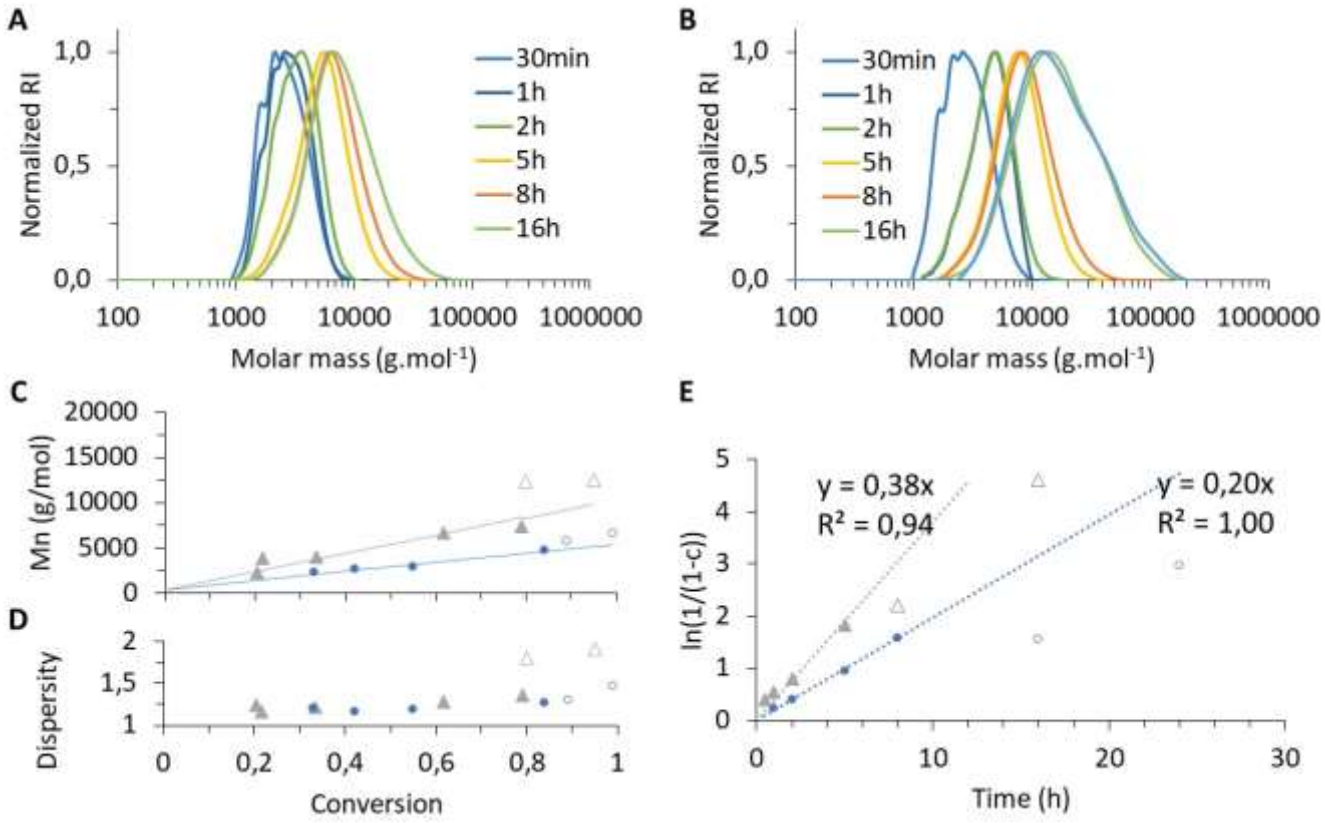

Figure 1. Chromatography trace of the kinetic [M]/[I] of 14 (A) and [M]/[I] of 27 (B) of the azomonomer "A"; Number-average molecular weight versus conversion, solid line represents the theoretical molecular weight (C); Dispersity versus conversion (D) and logarithmic of conversion against time of polymerization (E); circle blue: [M]/[I] of 14 and triangle grey: [M]/[I] of 27.

The logarithm of the conversion evolves linearly *versus* the polymerization time (Figure 1E) and the theoretical molecular weights fit well the experimental number-average molecular weights until 80 % conversion (Figure 1C). After 80 % of conversion, the polymerization starts to become less-controlled and the dispersity values increase with a wideness of the molecular weight distribution and shoulder (Figure 1B and D). In the same time, the logarithmic values of the conversion become lower than the theoretical ones (Figure 1E) that means the appearance of dead chains due to termination reaction.

In the literature, few azopolymers with high molecular weight, *i.e.* > 10-15kD, are obtained. Indeed, Cieciórski *et al.*[36] tried to optimize the synthesis of homopolymers of azobenzene by ATRP in 2021. Despite all their attempts with prolonged time of polymerization from 24 to 140 h or high [M]/[I] value ratio from 50 to 100, a maximum molecular weight was reached around 15 000 g.mol^{-1}. Wu and coll.[32] synthetized homopolymers of azobenzene by RAFT polymerization (9 900 g.mol^{-1}, $Đ$ = 1.32) and in order to achieve higher molecular weight, they used a preparative cycling SEC to obtain a molecular weight of 27 000 g.mol^{-1} with a dispersity value of 1.07. In another work,[42] they synthesized an azopolymer at 21 300 g.mol^{-1} with a dispersity of 1.37 by Cu(0)-RDRP. This difficulty to produce a homoazopolymer with a high molecular weight is the most often attributed to a strong steric hindrance or to the propagating radical which could interact with the azo group and then inhibit the polymerization.[46]

In order to analyze the effect of the nature and the size of the azopolymer chain, different kinds of azopolymers were synthesized (Table 1).

Table 1. Experimental conditions and features of Azopolymers.

Name	Monomer	Polymerization Time (h)	[M]/[I][a]	Conv (%)[b]	Mn_{theo} (g.mol^{-1})[c]	Mn_{exp} (g.mol^{-1})[d]	$Đ$[e]	Tg (°C)[f]
PA1	A	7	7	93	2 800	3 400	1.2	44
PA2	A	16	10	96	4 000	4 900	1.4	48
PA3	A	3.5	27	56	6 000	5 900	1.2	55
PA4	A	16	27	95	9 800	8 100	1.3	58
PB1	B	16	10	92	4 300	6 000	1.3	57
PB2	B	16	27	97	11500	11 400	1.4	61
PC	C	16	10	100	4 700	7 100	1.4	31
PD	D	16	10	100	4 900	7 400	1.3	60

[a] Molar ratio of monomer (M) and initiator (I); [b] conversion determined by ^{1}H NMR; [c] theoretical molecular weight determined from the conversion; [d] number-average molecular weight determined from SEC with PS calibration; [e] dispersity (Mw/Mn) determined by SEC, [f] Tg of the trans form determined by DSC.

If we decided to push the conversion, *i.e.* higher than 90 %, for recovering the largest amount of polymers from the introduced monomers, the final dispersity values remained nevertheless relatively low and comprised between 1.2 to 1.4 due to the precipitation recovery process.

In order to enhance the chain length of the azopolymer the initial [M]/[I] value ratio was increased up to 109 (Figure S5 and Table S1 in SI "part 2") but these experiments were unsuccessful.

Another option was to performed the NMP polymerization in DMF under microwave-assisted process (Table 2).[47]

Table 2. Polymerization features and characteristics of azopolymer prepared from monomer "A" under microwave irradiation

Name	[M]/[I] [a]	[M] (mol.L^{-1})	Time (min)	Cv [b]	Mn_{theo} [c]	Mn_{exp} [d]	$Đ$ [e]
« 1 »	14	0.15	30	44	2 600	2 300	1.15
« 2 »	27	0.53	30	59	6 300	3 700	1.18
« 3 »	109	0.78	15	25	10 200	4 400	1.14
« 4 »	109	0.78	30	30	12 500	4 200	1.15
« 5 »	109	0.78	60	23	9 700	4 400	1.15
« 6 »	109	1.21	30	31	12 900	5 700	1.19
« 7 »	219	1.68	30	17	14 300	6 900	1.19

[a] Molar ratio of monomer (M) and initiator (I); [b] conversion determined by ^{1}H NMR; [c] theoretical molecular weight determined from the conversion in g.mol^{-1}; [d] number-average molecular weight determined from SEC with PS calibration in g.mol^{-1}; [e] dispersity determined by SEC.

However, with this method, conversion was limited (< 59 %) and the highest molecular mass was 6 900 g.mol^{-1}. The effect of the microwave is still open and the reason for the increase in the polymerization rate (*Rp*) is under debate. Basically, two alternatives have been proposed: 1) one attributes the increase in *Rp* to thermal effects, which means rapid heating of the polymerization mixture and formation of super-heated regions. This case can be clearly observed where polymerization rate increases and a number of experimental results clearly demonstrate this scenario [48–50]. 2) The alternative idea is based on non-thermal effects, *i.e.* the effect of the microwave irradiation on the kinetic rate coefficients. This scenario is not widely accepted, but there are data in literature[47,51–53] that are difficult to explain in the absence of non-thermal effects[54]. In a small number of these cases a non-thermal effect has been claimed[54].

Independent of the mechanistic reason for the increase of the polymerization rate, the increase can be advantageously used to reduce the process time. Indeed, the polymerization time is highly reduced from hours to minutes. Indeed, we can highlight the experiment "3" where an azopolymer with a molecular weight of 4 400 g.mol^{-1} with a low dispersity (1.14) is obtained for a reaction time of 15 min, in comparison with 3 h under thermal activation.

2.3 *Reversible photoisomerization and stability behavior in solution*

2.3.1 Identification of cis and trans isomers.

The isomerization behavior of hydroxy-azobenzene compounds and azopolymers were first studied by ^{1}H NMR in $CDCl_3$. This technique was chosen instead of UV-visible spectrophotometry because it allows the direct reading of the proportion of the *cis/trans* forms without calibration steps. For small molecules such as hydroxy-azobenzenes and azomonomers, NMR peaks are well defined (Figure 2). ^{1}H NMR analysis of azobenzene like molecules in the *trans* form is common,[42] and peaks are well attributed. For *cis* isomers the peak identification is more difficult and scarcely presented in the literature. In order to attribute the ^{1}H NMR peaks of the *cis* isomers COSY NMR (Figure S6 in SI "part 2") and HMBC (Figure S7 in SI "part 2") allowing to respectively observe coupling between neighboring protons and between carbon and proton in *J2* and *J3* were performed to attribute correctly all the observed peaks (Figure 2). Characteristic peaks due to the *cis* isomer are shielded (7.1, 6.9, 6.8 and 6.7 ppm) by comparison with the *trans* isomer (7.9, 7.8, 7.3 and 7.0 ppm), each peak representing 2 protons due to the symmetry. As usual feature of the polymeric state, for the azopolymers, assigned peaks are widened. Apart from this broadening, the chemical shifts of the aromatic protons of the azopolymers follow the same trend as their precursor's counterparts. Due to the nearly symmetric nature of species "d and PD", the ^{1}H NMR attribution is different and represented in supplementary data (figure S8 in SI "part 2").

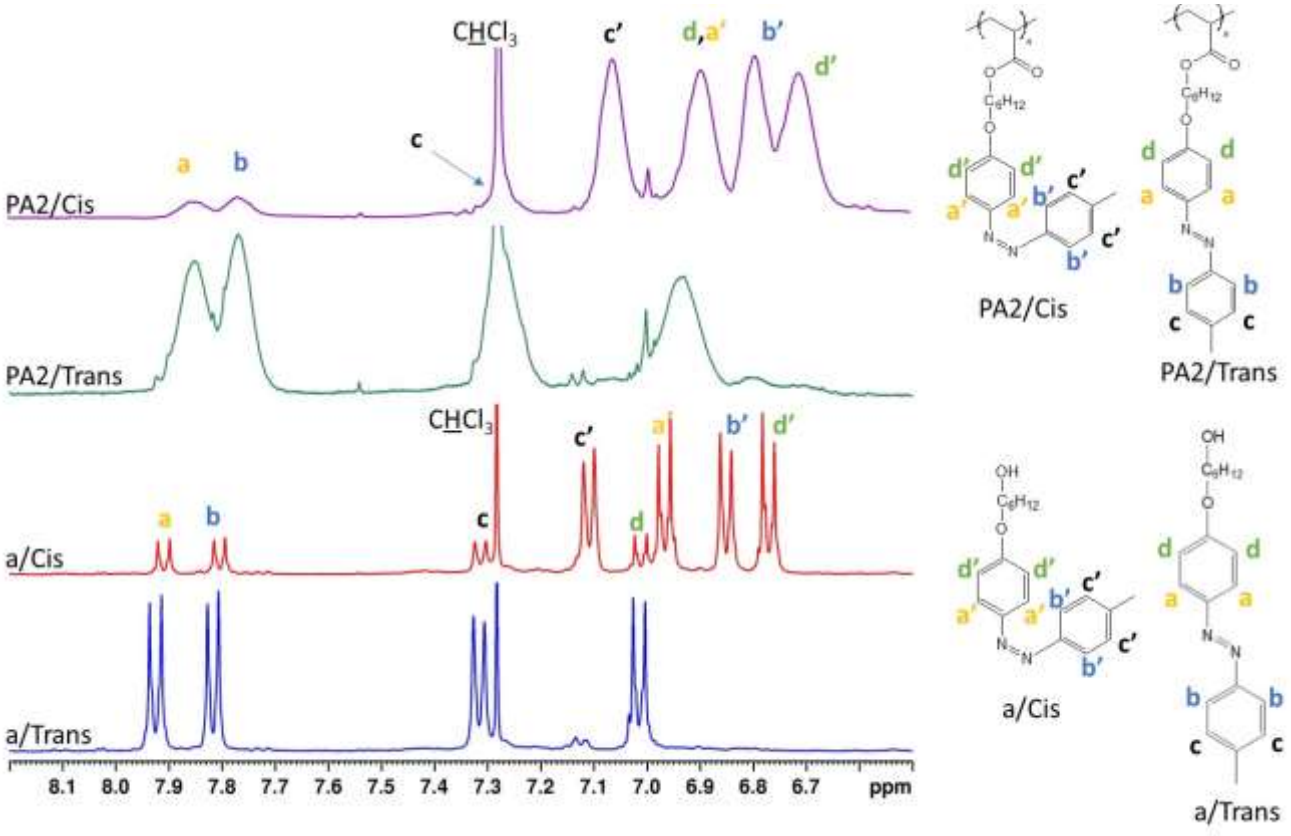

Figure 2. Aromatic area of ^{1}H NMR spectra of the *cis* and *trans* isomers of hydroxyazobenzene "a" and azopolymer "PA2".

2.3.2. *Trans* to *cis* Isomerization under UV.

An example of kinetic following the isomerization under 0.1 W/cm² UV light of an azopolymer using ^{1}H NMR in $CDCl_3$ and all half time of the *trans* isomer of all species are represented Figure 3.

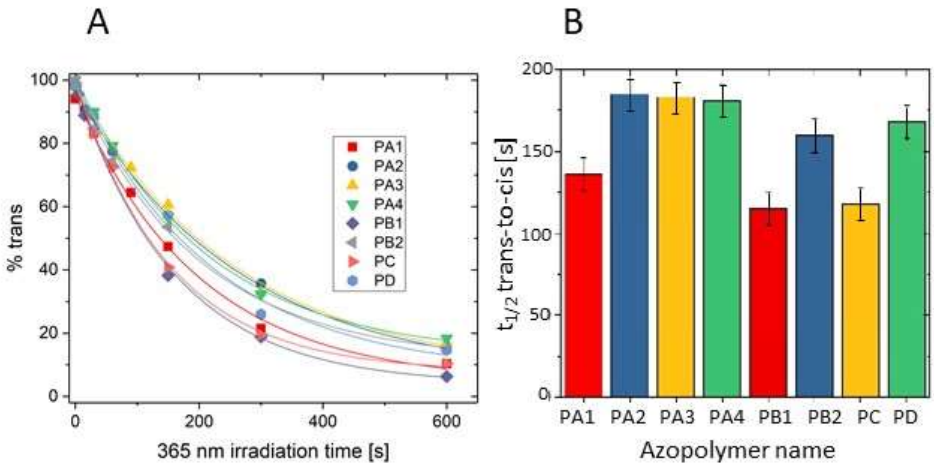

Figure 3. Percentage of *trans* isomer of the different azopolymers as function of the time under irradiation at 365 nm (A). Histogram representing the *trans* half-life time in seconds calculated from a 1st order kinetic model (B).

In the case of the *trans*-to-*cis* isomerization, the kinetic follows as expected a 1st order law.[55] As shown by Figure 3, the *trans*-to-*cis* isomerization is fast since the half-life time of the *trans* isomer varied between 110 and 185 seconds for the irradiation power used in the study. Increase of the chain length from PA1 to PA4 and PB1 to PB2 seems to slow down the speed of the *trans*-to-*cis* isomerization. Even if, it is known that the chemical structure seems to have a relative impact on the *trans*-to-*cis* isomerization process [56,57] for a similar Mn (PA3, PB1, PC and PD), *trans*-to-*cis* isomerization of PB1 and PC is faster. By comparing the chemical structure of these polymers, one can suppose that the presence of longer alkyl chain on the *para* position of the azo group, *i.e.* PC compared to PA3, leads to a relative increase of the *trans*-to-*cis* isomerization speed. This effect may be due to an increase of the steric effect or an increase of the inductive electron donor capacity. Oppositely the presence of a mesomeric electron-donor group, *i.e.* ether function, for PD compared to PC, leads to the opposite effect. The increase of the length of the alkoxy-linker, between PB1 and PA3, seems to increase the rate of the *trans*-to-*cis* isomerization in solution.

2.3.3 Stability of the cis isomer.

The rate of the thermal *cis*-to-*trans* isomerization is known to be determined by the mechanism through which the process takes place (inversion, rotation or mixed mechanism).[57] As shown in Figure 4, for all polymers the *cis*-to-*trans* thermal isomerization followed also a first order kinetic.[55] Because solution concentration has an important effect on the *cis* half-life time value (Figure S9 in SI "part 2"), we compared azopolymer solution with the same concentration (8.3 $g.l^{-1}$). The molecular weight has no significant effect on the *cis-to-trans* kinetic rate in solution in this range of macromolecular length (Figure 4A). As shown by Figure 4B, the thermal *cis*-to-*trans* photo-isomerization rate slowed down upon increasing the hydrophobic chain length (PC). This result is consistent with the results reported by Chen *et al.*[58] Increasing the steric hindrance of the alkyl chain

substituent in the para position may raises the height barrier of the inversion *cis-to-trans* mechanism. However, as it was already observed for azobenzene molecules, the presence of a mesomeric electron donor, *i.e.* for PD, seems to cancel this effect.[59]

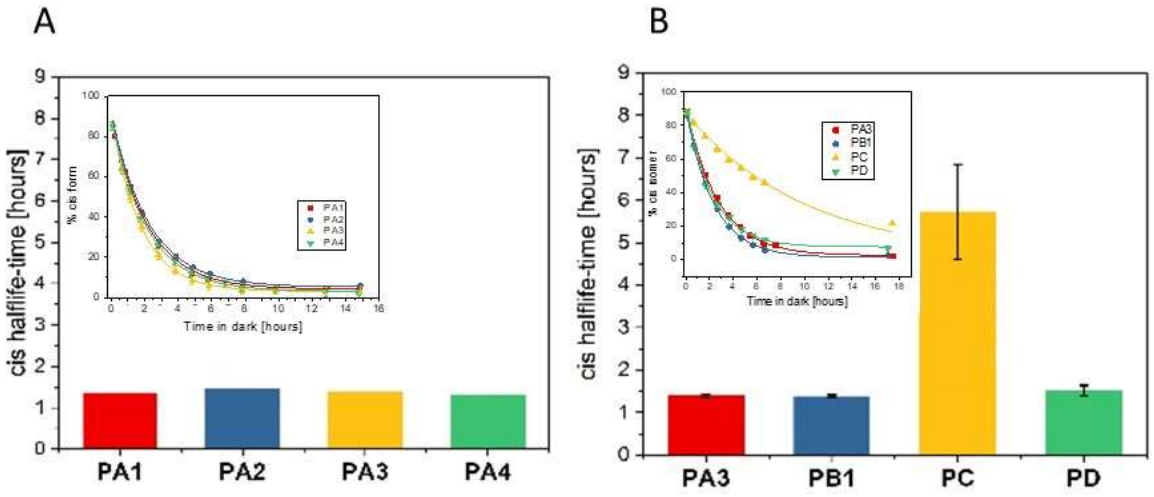

Figure 4. Evolution of the cis isomer percentage of azopolymers as function of the time in the dark regarding (A) the effect of the molecular weight with PA1, PA2, PA3 and PA4 (A) and (B) the effect of the nature of the azobenzene with PA3, PB1, PC and PD. Azopolymer (Azopolymer are initially irradiated at 365 nm to obtained the cis isomer. Inset represents the cis-half time in hour of the cis isomer calculated with a 1st order kinetic model).

We have shown that the photo-isomerization behavior of azopolymers is impacted by the chromophore structure and particularly by the size and the electron-donor capacity of the substitutes.

2.4 Photoinduced solid-to-liquid properties of azopolymers.

Under UV irradiation, some azopolymers can demonstrate a solid-to-liquid transition.[32] Table 3 shows the observed solid-to-liquid S→L transition under an optical microscope of the series of synthesized azopolymers when illuminated at 365 nm with an irradiance of 0.34 W.cm^{-2}.

Table 3. Optical microscopy images (350x270 µm²) and irradiation time of the reversible S→L transition and glass transition temperature measured by DSC of the cis isomer for the synthetized azopolymers

Azopolymer	Pristine *trans* form	15 s of irradiation (365 nm – 0.34W.cm^{-2})	Liquid phase (irradiation 365nm t>120s)	S→L transition irradiation time	Tg *cis* [°C]	After 4 days in the dark
PA1				30 s	31	
PA2				45 s	45	
PA3				45 s	44	
PA4				45 s	42	
PB1				30 s	38	
PB2				60 s	50	
PC			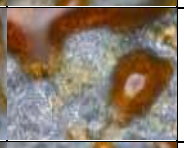	15 s	31	
PD	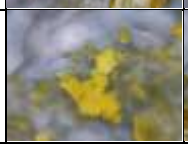	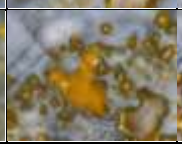		30 s	44	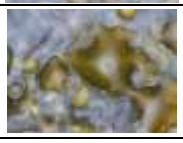

For all the azopolymers, we can observe a two-step mechanism for the S→L transition. At first, for short irradiation time, *i.e.* t = 15 s, a transition from yellowish to reddish color is observed without apparition of a liquid phase. This change of color can be attributed to the *trans*-to-*cis* isomerization of the azopolymer. Indeed, as shown in Figure 5, upon UV irradiation, the π–π* absorption band of *trans* azobenzene groups at ≈ 350 nm decreased. Correspondingly, the n–π* absorption band of the *cis* isomer at ≈ 450 nm increased with the irradiation time. The fast *trans*-to-*cis* isomerization observed in the solid phase confirms our results obtained in solution. In a second step, with prolonged irradiation, all the synthetized polymers show an S→L transition at an irradiation time depending of the polymer nature. At present, for azopolymers the S→L transition under irradiation is explained by the fact that the *trans*-to-*cis* isomerization decreases the glass transition temperature *Tg* of the material.[37]

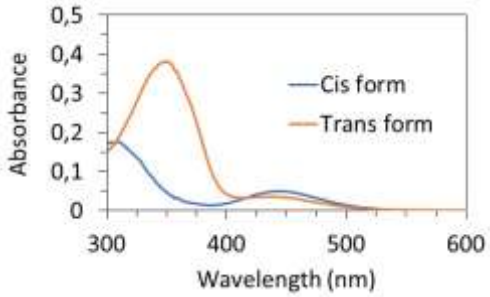

Figure 5. Representative UV-visible spectra of *cis* and *trans* forms for azopolymers (herein PA2).

Since the change of color of the azopolymers, *i.e. trans*-to-*cis* isomerization, occurred before the S→L transition, we suspect that the Tg_{cis} of our azopolymers are above room temperature and that a supplementary heating is needed to exceed the Tg_{cis} and cause the S→L transition. The increase of the material temperature can be provided by increasing the irradiation time. Therefore, the higher the Tg_{cis} of the material, the longer the irradiation time will be. The quantification of the amount of heat that has to be brought to the different azopolymer for the S→L transition occurrence is not in the aim of the present study and will be reported in a future publication.

To evaluate the effect of the molecular weight on the S→L transition, we can compare PA1 to PA4 and PB1 to PB2 azopolymers. For these polymers, an increase in molecular weight leads to longer irradiation time needed to make the S→L transition. As confirmed by the measured value of Tg_{cis} (Table 3) we believe that the observed longer irradiation time observed for the S→L transition for azopolymer with higher Mn can be explained by the increase of Tg_{cis}.

Concerning the effect of the molecular composition of the chromophore, if we compare PA3 with PB1, PC and PD with similar molecular weights, we can see that the S→L transition is faster for PB1, PC and PD than for PA3. For these polymers either the linker (PB1) or the *para*-substituent (PC, PD) are longer than those of PA3. We believe that the resulting enhanced flexibility leads to a decrease of the Tg_{cis} (Table 3) and thus a faster S→L transition. Concerning the linker length, our result agrees with those of Wu *et al.*,[37] and Akiyama *et al.*[38] showing that S→L transition at room temperature was only observable with higher alkyl length for azopolymer with a structure similar to that of our PA, PB and PC series. When we compare PC and PD, we can see that the S→L transition is faster for PC. Here we believe that the molecular structure of PD leads to a higher rigidity of the polymeric chain and thus a higher Tg_{cis} (*i.e.* 44°C) compared to PC (*i.e.* 31°C).

2.5 Reversibility of the S→L transition.

As shown on Table 3, four days in the dark are needed for all the azopolymers to recover their yellowish color characteristic of the *trans* form. This result agrees with the good stability of the *cis* form observed in solution (Figure 4). After 4 days in the dark the azopolymers have also recovered their initial solid property (Figure 6).

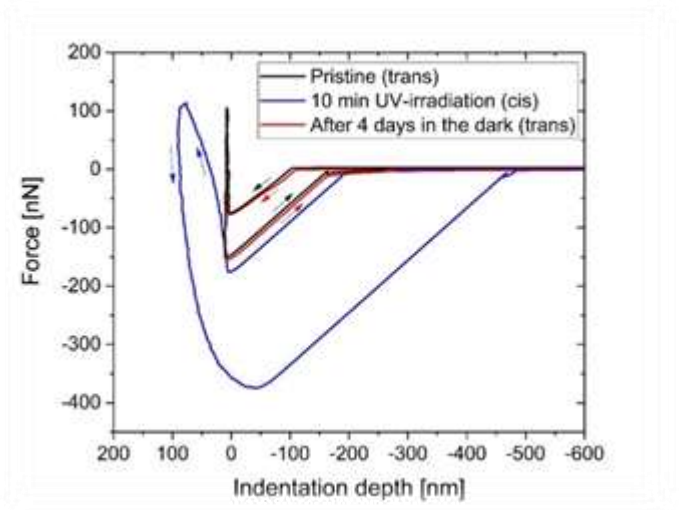

Figure 6. Representative AFM force-distance curve on PA3 before and after irradiation, and for 4 days in the dark. Arrows indicate the direction of the AFM scanner toward the sample (*i.e.* approach and retraction)

Atomic Force Microscopy (AFM) force-distance curves representative of the pristine PA3 material (trans form) are characterized by a weak hysteresis between the approach and retraction phases, a low adhesion (*i.e.* maximum negative force) and high slope in the region of positive indentation (*i.e.* high rigidity). These curves are characteristic of a solid-like behavior of polymeric material.[60] In comparison the curves, obtained after 10 min of UV irradiation (*i.e.* when the S→L transition is complete) show a high hysteresis between the approach and retracting curves characteristic of a viscous fluid.[60] Finally, when the liquid-like sample is kept in the dark for four days the force distance curves return to their original shape which demonstrate the reversibility of the S→L transition.

3. Conclusion

In this study, in order to understand the structure–property relationship on photoinduced solid-to-liquid transition properties, Nitroxide Mediated Polymerization was used to synthesize well-defined azopolymers. Four acrylate monomers (A, B, C and D) were designed and then polymerized. Four different molecular weight, *i.e*. from 3 400 to 8 100 g.mol^{-1} were targeted for the "A" monomer C_6H_{12}-azo-CH_3. Higher molecular weights are not reachable, even under micro-assisted polymerization, because of the steric hindrance of the monomer. Photo-isomerization properties and photo-reversible solid-to-liquid transitions were studied as function of the molecular weight and the molecular structure of the azopolymers. Both have an impact on the features of the reversible solid-to-liquid transition. In particular, the higher the length of the substituent or the linker, the faster the transition. This is due to a gain in flexibility of the side chain that leads to a decrease in the Tg value of the *cis* form. These results have to be considered in the design of novel azopolymers for practical applications.

4 Experimental Section

4.1 Materials

Triethylamine (99 %, ABCR), 4-Dimethylaminopyridine (≥ 99 %, DMAP, Sigma-Aldrich), Acrylic Anhydride (> 95 %, TCI) were used without purification. The BlocBuilder® alkoxyamine (2-methylaminoxypropionic-SG1) used as the initiator was supplied by Arkema. All solvents and Dialysis Membrane (Spectra/Por® 6 pre-wetted RC Tubing, MWCO: 2 kD) were purchase from VWR and used as received. Dry THF was dried using a PureSolv (INERT) solvent purification system under N_2.

4.2 Synthesis

Synthesis of hydroxy-azobenzene. Four different hydroxy-azobenzenes (Figure 7) were synthetized and characterized following the method described in supplementary data "Part 1".

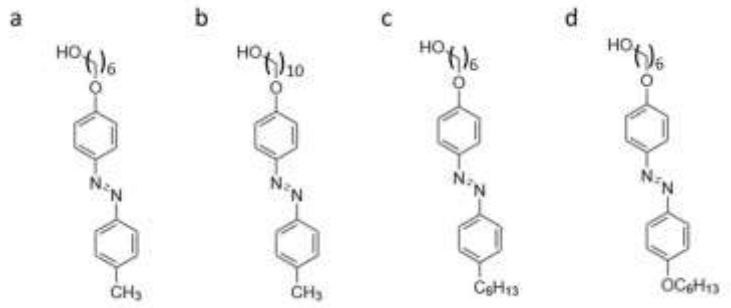

Figure 7. Denominations of the hydroxy-azobenzene precursors synthetized: (a) HO-C_6H_{12}-azo-CH_3, (b) HO-$C_{10}H_{20}$-azo-CH_3, (c) OH-C_6H_{12}-azo-C_6H_{13} and (d) HO-C_6H_{12}-azo-OC_6H_{13}.

Synthesis of azomonomer. All azomonomers were prepared using the same method (Table 4). Hydroxy-azobenzene (1 eq), anhydride acrylic (1.5 eq), triethylamine (1.2 eq), 4-dimethylaminopyridine (0.3 eq) are mixed in dry THF and degassed during 15 min. The reactional mixture was heated at 40°C during 24 h. To purify the monomer, the solution is filtered and then washed by precipitation in water (2 times). To finish, the powder is dried under vacuum at 30°C. Azomonomers were characterized by ^{1}H NMR in $CDCl_3$ (supplementary data Figure S1 to S4 "part 2").

Table 4. Experimental conditions for azomonomer synthesis.

AzoMonomer	$M_{OH\text{-}azo}$[a] (g.mol^{-1})	[OH-azo] (mol.L^{-1})	$n_{OH\text{-}azo}$ (mmol)	% Yield[b]
A: $C_6H_{12}O$-azo-CH_3	312	3.2 x 10^{-4}	12.8	90
B: $C_{10}H_{20}O$-azo-CH_3	368	2.7 x 10^{-4}	2.72	91
C: $C_6H_{12}O$-azo-C_6H_{13}	382	2.6 x 10^{-4}	7.9	75
D: $C_{10}H_{20}O$-azo-OC_6H_{13}	398	2.6 x 10^{-4}	7.6	82

[a] OH-azo = hydroxyazobenzene, [b] Yield after purification.

Synthesis of azopolymer by NMP. Azopolymers were synthetized using the same protocol. For example, to obtain an azopolymer PA3 with an initial [M]/[I] equal to 27, 0.5 g of azomonomer C_6H_{12}-azo-CH_3 (366 g.mol^{-1}, 1.36 mmol) and 19.3 mg of BlocBuilder® (381 g.mol^{-1}, 0.05 mmol) were mixed, degassed during 10 min and heating at 115°C during 16 h. The final solution was analyzed by ^{1}H NMR before purification, in this case 95 % of conversion were obtained. After purification by dialysis in a mixture of THF, ethanol and water, the purified sample is analyzed by ^{1}H NMR and SEC in THF. The obtained number-average molecular weight was 8 100 g.mol^{-1} with a dispersity of 1.27.

Synthesis of azopolymer by NMP using microwave reactor. Experimental conditions for entry 2 in table 2 with an initial [M]/[I] equal to 27 is given as an example. 60 mg of azomonomer A (366 $g.mol^{-1}$, 164 µmol) and 2.3 mg of BlocBuilder® (381 $g.mol^{-1}$, 6 µmol) were mixed in 0.25 mL of DMF and degassed during 10 min. Then, the mixture is exposed to microwave at 300 W using the SPS mode with a limit of temperature at 115 ± 1°C. After the exposition, ^{1}H NMR and SEC analysis were realized. In this case, the conversion was 59 % and the final number-average molecular weight was 3 700 $g.mol^{-1}$ with a dispersity of 1.18.

Photo-isomerization experiments. Irradiation of solutions and powder were performed at 365 nm with a High-Power LED from ThorLabs (SOLIS-365C). Irradiance was controlled at 0.10 $W.cm^{-2}$ and 0.34 $W.cm^{-2}$ for solution and powder respectively.

4.3 Characterization

The molecular weight and dispersity values of polymers were measured using size exclusion chromatography (SEC) using THF as eluent (flow rate 1.0 $mL.min^{-1}$) at 35°C. SEC is equipped with a Viscotek VE 5200 automatic injector, a pre-column and two columns (Styragels HR 5E and 4E (7.8´ 300 mm), an orbit wyatt and 4 detectors: UV-visible spectrophotometer (Viscotek VE 3210), a Multi-angle Light Scattering detector (Wyatt Heleos II), a viscosimeter (Viscostar Neon Wyatt) and a refractive index detector (Viscotek VE 3580). Number-average molar mass (Mn) and dispersity (Mw/Mn, where Mw is the mass-average molar mass) of the polymers were calculated from a calibration derived from polystyrene standards. The polymer samples were prepared at 5 $g.L^{-1}$ and filtered through 0.45 µm PTFE filters.

^{1}H NMR, COSY and HMBC experiments were carried out on a Bruker AVANCE 400 MHz spectrometer in $CDCl_3$ at 25°C. Chemical shifts were reported as ppm downfield from TetraMethyl Silane (TMS). The polymer solution in $CDCl_3$ were prepared at 8.3 $g.L^{-1}$.

UV-visible absorbance of polymers was measured on a double-beam spectrophotometer (Cary 5000, Varian). Spectra were recorded at room temperature in the range 250−700 nm.

Glass transition temperature (Tg) were measured with Differential scanning calorimetry (DSC) METTLER TOLEDO DSC 3 at 20°C.min^{-1}. Two cycles of temperature were realized to -10°C to 150°C to -10°C. The value of the Tg of the second cycle was chosen for the Tg of the *trans* isomer. After these two cycles, samples were irradiated 30 min under 365 nm and then analyzed again between -10°C to 150°C at 20°C.min^{-1} in order to obtain the Tg of the *cis* isomer. The STAR^{e} software was using for DSC treatment.

The irradiation time was measured as the time from which the liquefaction of the powder is observed by optical microscopy (x20 objective) when the material is subjected to irradiation at 100 mW/cm².

Acknowledgements

We gratefully acknowledge Brewen le Floch for the synthesis of hydroxy-azobenzene, Sullivan Bricaud and Abdel Khoukh for COSY and HMBC NMR analyses, and Alexandre Bénard for the HRMS analyses.

The ANR-20-CE06-0014-01 (Photoprint) for funding.

CRediT authorship contribution statement

Laurence Pessoni: Investigation, Writing original draft, Review & editing, **David Siniscalco:** Investigation, **Anne Boussonnière:** Writing review, **Anne-Sophie Castanet:** Writing review, **Nicolas Delorme:** Supervision, Writing review, Funding acquisition, **Laurent Billon:** Supervision, Writing review.

Declaration of Competing Interest

The authors declare that they have no known competing financial interests or personal relationships that could have appeared to influence the work reported in this paper.

Data availability statement

The raw/processed data required to reproduce these findings cannot be shared at this time as the data also forms part of an ongoing study.

References

[1] X. Huang, Y. Sun, S. Soh, Stimuli-Responsive Surfaces for Tunable and Reversible Control of Wettability, Advanced Materials. 27 (2015) 4062–4068. https://doi.org/10.1002/adma.201501578.

[2] Y. Ye, J. Huang, X. Wang, Fabrication of a Self-Cleaning Surface via the Thermosensitive Copolymer Brush of P(NIPAAm-PEGMA), ACS Applied Materials and Interfaces. 7 (2015) 22128–22136. https://doi.org/10.1021/acsami.5b07336.

[3] P. Marcasuzaa, H. Yin, Y. Feng, L. Billon, CO2-Driven reversible wettability in a reactive hierarchically patterned bio-inspired honeycomb film, Polymer Chemistry. 10 (2019) 3751–3757. https://doi.org/10.1039/c9py00488b.

[4] H. Yin, F. Zhan, Z. Li, H. Huang, P. Marcasuzaa, X. Luo, Y. Feng, L. Billon, CO2-Triggered ON/OFF Wettability Switching on Bioinspired Polylactic Acid Porous Films for Controllable Bioadhesion, Biomacromolecules. 22 (2021) 1721–1729. https://doi.org/10.1021/acs.biomac.1c00134.
[5] P. Marcasuzaa, M. Save, P. Gérard, L. Billon, When a pH-triggered nanopatterned shape transition drives the wettability of a hierarchically self-organized film: A bio-inspired effect of "sea Anemone," Journal of Colloid and Interface Science. (2021). https://doi.org/10.1016/j.jcis.2020.07.130.
[6] M.D. Manrique-Juárez, S. Rat, L. Salmon, G. Molnár, C.M. Quintero, L. Nicu, H.J. Shepherd, A. Bousseksou, Switchable molecule-based materials for micro- and nanoscale actuating applications: Achievements and prospects, Coordination Chemistry Reviews. 308 (2016) 395–408. https://doi.org/10.1016/j.ccr.2015.04.005.
[7] W. Horspool, F. Lenci, CRC handbook of: Organic photochemistry and photobiology, second edition, 2003. https://www.scopus.com/inward/record.uri?eid=2-s2.0-85056335236&partnerID=40&md5=272a07d7865ee30054581b1802f0dc48.
[8] H. Dürr, H. Bouas-Laurent, Photochromism: Molecules and systems, 2003. https://doi.org/10.1016/B978-0-444-51322-9.X5000-3.
[9] H. Rau, E. Lüddecke, On the Rotation-Inversion Controversy on Photoisomerization of Azobenzenes. Experimental Proof of Inversion, J Am Chem Soc. 104 (1982) 1616–1620. https://doi.org/10.1021/ja00370a028.
[10] M. Gondry, C. Dugave, Other Cis-Trans Isomerizations in Organic Molecules and Biomolecules, in: Cis-Trans Isomerization in Biochemistry, 2006: pp. 295–320. https://doi.org/10.1002/9783527609338.ch13.
[11] X. Wang, Azo Polymers, Springer Berlin Heidelberg, Berlin, Heidelberg, 2017. https://doi.org/10.1007/978-3-662-53424-3.
[12] W. Ji, Q. Wu, X. Han, W. Zhang, W. Wei, L. Chen, L. Li, W. Huang, Photosensitive hydrogels: from structure, mechanisms, design to bioapplications, Science China Life Sciences. 63 (2020) 1813–1828. https://doi.org/10.1007/s11427-019-1710-8.
[13] H.-B. Cheng, S. Zhang, J. Qi, X.-J. Liang, J. Yoon, Advances in Application of Azobenzene as a Trigger in Biomedicine: Molecular Design and Spontaneous Assembly, Advanced Materials. 33 (2021). https://doi.org/10.1002/adma.202007290.
[14] Y.-B. Wei, Q. Tang, C.-B. Gong, M.H.-W. Lam, Review of the recent progress in photoresponsive molecularly imprinted polymers containing azobenzene chromophores, Analytica Chimica Acta. 900 (2015) 10–20. https://doi.org/10.1016/j.aca.2015.10.022.
[15] H. Kim, S.-K. Ahn, D.M. Mackie, J. Kwon, S.H. Kim, C. Choi, Y.H. Moon, H.B. Lee, S.H. Ko, Shape morphing smart 3D actuator materials for micro soft robot, Materials Today. 41 (2020) 243–269. https://doi.org/10.1016/j.mattod.2020.06.005.
[16] Y. Yu, M. Nakano, T. Ikeda, Directed bending of a polymer film by light, Nature. 425 (2003) 145. https://doi.org/10.1038/425145a.
[17] T. Ikeda, O. Tsutsumi, Optical switching and image storage by means of azobenzene liquid-crystal films, Science (1979). 268 (1995) 1873–1875. https://doi.org/10.1126/science.268.5219.1873.
[18] H.M. Colquhoun, Self-repairing polymers: Materials that heal themselves, Nature Chemistry. 4 (2012) 435–436. https://doi.org/10.1038/nchem.1357.
[19] S. Wu, H.-J. Butt, Solar-Thermal Energy Conversion and Storage Using Photoresponsive Azobenzene-Containing Polymers, Macromolecular Rapid Communications. 41 (2020). https://doi.org/10.1002/marc.201900413.
[20] A. Priimagi, A. Shevchenko, Azopolymer-based micro- and nanopatterning for photonic applications, Journal of Polymer Science, Part B: Polymer Physics. 52 (2014) 163–182. https://doi.org/10.1002/polb.23390.
[21] T. Ikeda, J.-I. Mamiya, Y. Yu, Photomechanics of liquid-crystalline elastomers and other polymers, Angewandte Chemie - International Edition. 46 (2007) 506–528. https://doi.org/10.1002/anie.200602372.
[22] S. Palagi, A.G. Mark, S.Y. Reigh, K. Melde, T. Qiu, H. Zeng, C. Parmeggiani, D. Martella, A. Sanchez-Castillo, N. Kapernaum, F. Giesselmann, D.S. Wiersma, E. Lauga, P. Fischer, Structured light enables biomimetic swimming and versatile locomotion of photoresponsive soft microrobots, Nature Materials. 15 (2016) 647–653. https://doi.org/10.1038/nmat4569.
[23] B. Xu, C. Zhu, L. Qin, J. Wei, Y. Yu, Light-Directed Liquid Manipulation in Flexible Bilayer Microtubes, Small. 15 (2019). https://doi.org/10.1002/smll.201901847.
[24] S. Li, Z. Wu, M. Wang, S. Wu, Photoinduced healing of mechanically robust polymers, Chemistry Letters. 50 (2021) 7–13. https://doi.org/10.1246/CL.200548.
[25] G. Xu, S. Li, C. Liu, S. Wu, Photoswitchable Adhesives Using Azobenzene-Containing Materials, Chemistry - An Asian Journal. 15 (2020) 547–554. https://doi.org/10.1002/asia.201901655.

[26] W.-C. Xu, S. Sun, S. Wu, Photoinduced Reversible Solid-to-Liquid Transitions for Photoswitchable Materials, Angewandte Chemie - International Edition. 58 (2019) 9712–9740. https://doi.org/10.1002/anie.201814441.
[27] P. Weis, W. Tian, S. Wu, Photoinduced Liquefaction of Azobenzene-Containing Polymers, Chemistry - A European Journal. 24 (2018) 6494–6505. https://doi.org/10.1002/chem.201704162.
[28] T. Yamamoto, Y. Norikane, H. Akiyama, Photochemical liquefaction and softening in molecular materials, polymers, and related compounds, Polymer Journal. 50 (2018) 551–562. https://doi.org/10.1038/s41428-018-0064-4.
[29] B. Yang, M. Yu, H. Yu, Azopolymer-Based Nanoimprint Lithography: Recent Developments in Methodology and Applications, Chempluschem. 85 (2020) 2166–2176. https://doi.org/10.1002/cplu.202000495.
[30] L. Oscurato Stefano, M. Salvatore, P. Maddalena, A. Ambrosio, From nanoscopic to macroscopic photo-driven motion in azobenzene-containing materials, Nanophotonics. 7 (2018) 1387. https://doi.org/10.1515/nanoph-2018-0040.
[31] G.M. Kehe, D.I. Mori, M.J. Schurr, D.P. Nair, Optically Responsive, Smart Anti-Bacterial Coatings via the Photofluidization of Azobenzenes, ACS Applied Materials and Interfaces. 11 (2019) 1760–1765. https://doi.org/10.1021/acsami.8b21058.
[32] H. Zhou, C. Xue, P. Weis, Y. Suzuki, S. Huang, K. Koynov, G.K. Auernhammer, R. Berger, H.-J. Butt, S. Wu, Photoswitching of glass transition temperatures of azobenzene-containing polymers induces reversible solid-to-liquid transitions, Nature Chemistry. 9 (2017) 145–151. https://doi.org/10.1038/NCHEM.2625.
[33] Y. Yue, Y. Norikane, R. Azumi, E. Koyama, Light-induced mechanical response in crosslinked liquid-crystalline polymers with photoswitchable glass transition temperatures, Nature Communications. 9 (2018). https://doi.org/10.1038/s41467-018-05744-x.
[34] J. Xu, B. Niu, S. Guo, X. Zhao, X. Li, J. Peng, W. Deng, S. Wu, Y. Liu, Influence of chromophoric electron-donating groups on photoinduced solid-to-liquid transitions of azopolymers, Polymers (Basel). 12 (2020). https://doi.org/10.3390/POLYM12040901.
[35] S. Ito, A. Yamashita, H. Akiyama, H. Kihara, M. Yoshida, Azobenzene-Based (Meth)acrylates: Controlled Radical Polymerization, Photoresponsive Solid-Liquid Phase Transition Behavior, and Application to Reworkable Adhesives, Macromolecules. 51 (2018) 3243–3253. https://doi.org/10.1021/acs.macromol.8b00156.
[36] P. Cieciórski, P.W. Majewski, E. Megiel, New photoresponsive poly(Meth)acrylates bearing azobenzene moieties obtained via atrp polymerization exhibiting liquid-crystalline behavior, Polymers (Basel). 13 (2021). https://doi.org/10.3390/polym13132172.
[37] P. Weis, A. Hess, G. Kircher, S. Huang, G.K. Auernhammer, K. Koynov, H.-J. Butt, S. Wu, Effects of Spacers on Photoinduced Reversible Solid-to-Liquid Transitions of Azobenzene-Containing Polymers, Chemistry - A European Journal. 25 (2019) 10946–10953. https://doi.org/10.1002/chem.201902273.
[38] H. Akiyama, T. Fukata, A. Yamashita, M. Yoshida, H. Kihara, Reworkable adhesives composed of photoresponsive azobenzene polymer for glass substrates, The Journal of Adhesion. 93 (2017) 823–830. https://doi.org/10.1080/00218464.2016.1219255.
[39] N. Corrigan, K. Jung, G. Moad, C.J. Hawker, K. Matyjaszewski, C. Boyer, Reversible-deactivation radical polymerization (Controlled/living radical polymerization): From discovery to materials design and applications, Progress in Polymer Science. 111 (2020) 101311. https://doi.org/https://doi.org/10.1016/j.progpolymsci.2020.101311.
[40] M. Chen, B. Yao, M. Kappl, S. Liu, J. Yuan, R. Berger, F. Zhang, H.-J. Butt, Y. Liu, S. Wu, Entangled Azobenzene-Containing Polymers with Photoinduced Reversible Solid-to-Liquid Transitions for Healable and Reprocessable Photoactuators, Advanced Functional Materials. 30 (2020). https://doi.org/10.1002/adfm.201906752.
[41] L. Pessoni, N. Delorme, L. Billon, Light-triggered surface properties of a glycolized PolyEthylene Terephthalate film by surface-initiated ATRP of azobenzene monomer, European Polymer Journal. 156 (2021) 110608. https://doi.org/10.1016/j.eurpolymj.2021.110608.
[42] Z. Zhang, M. Chen, I. Schneider, Y. Liu, S. Liang, S. Sun, K. Koynov, H.-J. Butt, S. Wu, Long Alkyl Side Chains Simultaneously Improve Mechanical Robustness and Healing Ability of a Photoswitchable Polymer, Macromolecules. 53 (2020) 8562–8569. https://doi.org/10.1021/acs.macromol.0c01784.
[43] J. Nicolas, Y. Guillaneuf, C. Lefay, D. Bertin, D. Gigmes, B. Charleux, Nitroxide-mediated polymerization, Progress in Polymer Science. 38 (2013) 63–235. https://doi.org/10.1016/j.progpolymsci.2012.06.002.
[44] E. Yoshida, M. Ohta, Preparation of micelles with azobenzene at their coronas or cores from ‘nonamphiphilic’ diblock copolymers, Colloid and Polymer Science - COLLOID POLYM SCI. 283 (2005) 521–531. https://doi.org/10.1007/s00396-004-1179-z.

[45] S. Srichan, D. Chan-Seng, J.-F. Lutz, Influence of strong electron-donor monomers in sequence-controlled polymerizations, ACS Macro Letters. 1 (2012) 589–592. https://doi.org/10.1021/mz3001513.
[46] X. Wang, Azo Polymer Syntheses, in: X. Wang (Ed.), Azo Polymers: Synthesis, Functions and Applications, Springer Berlin Heidelberg, Berlin, Heidelberg, 2017: pp. 57–115. https://doi.org/10.1007/978-3-662-53424-3_3.
[47] P. Marcasuzaa, S. Reynaud, B. Grassl, H. Preud'Homme, J. Desbrires, M. Trchov, O.F.X. Donard, Microwave synthesis: An alternative approach to synthesize conducting end-capped polymers, Polymer (Guildf). 52 (2011) 33–39. https://doi.org/10.1016/j.polymer.2010.11.016.
[48] Y. Kwak, R.T. Mathers, K. Matyjaszewski, Critical evaluation of the microwave effect on radical (Co)polymerizations, Macromolecular Rapid Communications. 33 (2012) 80–86. https://doi.org/10.1002/marc.201100618.
[49] Y. Sugihara, M. Semsarilar, S. Perrier, P.B. Zetterlund, Assessment of the influence of microwave irradiation on conventional and RAFT radical polymerization of styrene, Polymer Chemistry. 3 (2012) 2801–2806. https://doi.org/10.1039/C2PY20434G.
[50] R.M. Paulus, C.R. Becer, R. Hoogenboom, U.S. Schubert, High temperature initiator-free RAFT polymerization of methyl methacrylate in a microwave reactor, Australian Journal of Chemistry. 62 (2009) 254–259. https://doi.org/10.1071/CH09064.
[51] S.L. Brown, C.M. Rayner, S. Graham, A. Cooper, S. Rannard, S. Perrier, Ultra-fast microwave enhanced reversible addition-fragmentation chain transfer (RAFT) polymerization: monomers to polymers in minutes, Chemical Communications. (2007) 2145–2147. https://doi.org/10.1039/B703386A.
[52] D. Roy, A. Ullah, B.S. Sumerlin, Rapid Block Copolymer Synthesis by Microwave-Assisted RAFT Polymerization, Macromolecules. 42 (2009) 7701–7708. https://doi.org/10.1021/ma901471k.
[53] J. Rigolini, B. Grassl, L. Billon, S. Reynaud, O.F.X. Donard, Microwave-assisted nitroxide-mediated radical polymerization of acrylamide in aqueous solution, Journal of Polymer Science, Part A: Polymer Chemistry. 47 (2009) 6919–6931. https://doi.org/10.1002/pola.23731.
[54] P.B. Zetterlund, S. Perrier, RAFT Polymerization under Microwave Irradiation: Toward Mechanistic Understanding, Macromolecules. 44 (2011) 1340–1346. https://doi.org/10.1021/ma102689d.
[55] H.M.D. Bandara, S.C. Burdette, Photoisomerization in different classes of azobenzene, Chemical Society Reviews. 41 (2012) 1809–1825. https://doi.org/10.1039/c1cs15179g.
[56] L. Schweighauser, M.A. Strauss, S. Bellotto, H.A. Wegner, Attraction or Repulsion? London Dispersion Forces Control Azobenzene Switches, Angewandte Chemie - International Edition. 54 (2015) 13436–13439. https://doi.org/10.1002/anie.201506126.
[57] J. García-Amorós, D. Velasco, Recent advances towards azobenzene-based lightdriven real-time information-transmitting materials, Beilstein Journal of Organic Chemistry. 8 (2012). https://doi.org/10.3762/bjoc.8.113.
[58] S. Chen, C. Wang, Y. Yin, K. Chen, Synthesis of photo-responsive azobenzene molecules with different hydrophobic chain length for controlling foam stability, RSC Advances. 6 (2016) 60138–60144. https://doi.org/10.1039/c6ra06459k.
[59] P.D. Maria, A. Fontana, C. Gasbarri, G. Siani, P. Zanirato, Kinetics of the Z-E isomerization of monosubstituted azobenzenes in polar organic and aqueous micellar solvents, Arkivoc. 2009 (2009) 16–29. https://doi.org/10.3998/ark.5550190.0010.803.
[60] N. Delorme, M.S. Chebil, G. Vignaud, V. le Houerou, J.-F. Bardeau, R. Busselez, A. Gibaud, Y. Grohens, Experimental evidence of ultrathin polymer film stratification by AFM force spectroscopy, The European Physical Journal E. 38 (2015) 56. https://doi.org/10.1140/epje/i2015-15056-9.

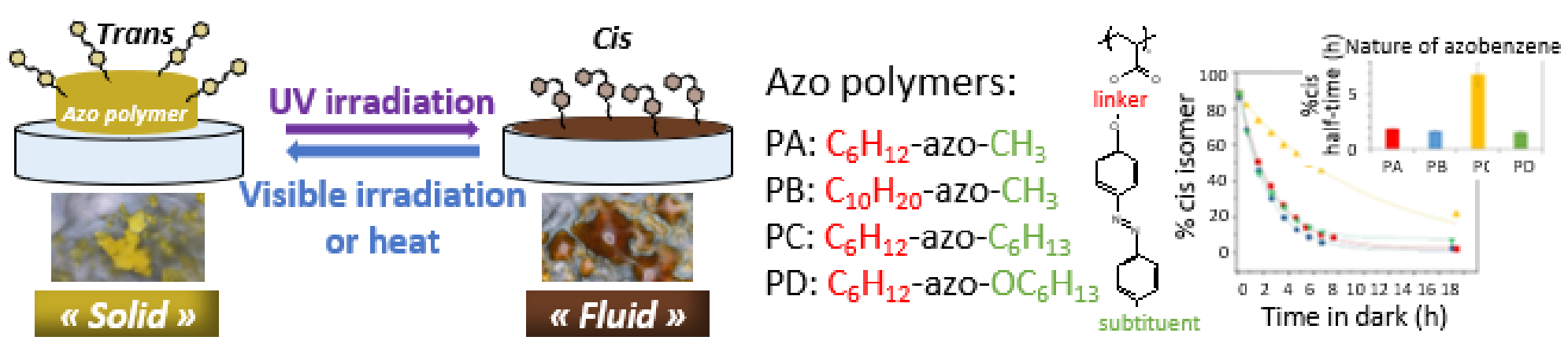
Trans
Azo polymer
« Solid »
UV irradiation
Visible irradiation
or heat
Cis
« Fluid »
Azo polymers:
PA: C6H12-azo-CH3
PB: C10H20-azo-CH3
PC: C6H12-azo-C6H13
PD: C6H12-azo-OC6H13
linker
subtituent
% cis isomer
Time in dark (h)
Nature of azobenzene
%cis half-time (h)
PA
PB
PC
PD